



HAL
open science

Phase-change radiative thermal diode

Philippe Ben-Abdallah, Svend-Age Biehs

► **To cite this version:**

Philippe Ben-Abdallah, Svend-Age Biehs. Phase-change radiative thermal diode. *Applied Physics Letters*, 2013, 103 (19), pp.191907. 10.1063/1.4829618]. hal-01334898

HAL Id: hal-01334898

<https://hal-iogs.archives-ouvertes.fr/hal-01334898>

Submitted on 21 Jun 2016

HAL is a multi-disciplinary open access archive for the deposit and dissemination of scientific research documents, whether they are published or not. The documents may come from teaching and research institutions in France or abroad, or from public or private research centers.

L'archive ouverte pluridisciplinaire **HAL**, est destinée au dépôt et à la diffusion de documents scientifiques de niveau recherche, publiés ou non, émanant des établissements d'enseignement et de recherche français ou étrangers, des laboratoires publics ou privés.

Phase-change radiative thermal diode

Philippe Ben-Abdallah^{1,a)} and Svend-Age Biehs^{2,b)}

¹Laboratoire Charles Fabry, UMR 8501, Institut d'Optique, CNRS, Université Paris-Sud 11, 2, Avenue Augustin Fresnel, 91127 Palaiseau Cedex, France

²Institut für Physik, Carl von Ossietzky Universität, D-26111 Oldenburg, Germany

(Received 10 July 2013; accepted 24 October 2013; published online 7 November 2013)

A thermal diode transports heat mainly in one preferential direction rather than in the opposite direction. This behavior is generally due to the non-linear dependence of certain physical properties with respect to the temperature. Here we introduce a radiative thermal diode which rectifies heat transport thanks to the phase transitions of materials. Rectification coefficients greater than 70% and up to 90% are shown, even for small temperature differences. This result could have important applications in the development of future contactless thermal circuits or in the conception of radiative coatings for thermal management. © 2013 AIP Publishing LLC. [<http://dx.doi.org/10.1063/1.4829618>]

Asymmetry of heat transport with respect to the sign of the temperature gradient between two points is the basic definition of thermal rectification,^{1,2} which is at the heart of a variety of applications as, for example, in thermal regulation, thermal modulation, and heat engines. This unusual thermal behavior has opened the way to new concepts for manipulating the heat flow similar to the electric current in electronic devices. Usually, this manipulation finds its origin in the non-linear behavior of materials with respect to the temperature, which, for the thermal rectification, breaks the symmetry of transfer when the temperature gradient is reversed. The effectiveness of the thermal rectification can be measured by means of the rectification coefficient $\eta = \frac{|\Phi_F - \Phi_R|}{\max(\Phi_F, \Phi_R)}$, where Φ_F and Φ_R denote the heat flux in the forward and reverse operating mode, respectively. Different solid-state thermal diodes have been conceived during the last decade from various mechanisms (see Ref. 3, for a review on phononic rectification), including nonlinear atomic vibrations,⁴ nonlinearity of the electron gas dispersion relation in metals,⁵ direction dependent Kapitza resistances,⁶ or dependence of the superconducting density of states and phase dependence of heat currents flowing through Josephson junctions.⁷

More Recently, photon-mediated thermal rectifiers^{8,9} have been proposed to tune near-field heat exchange using materials with thermally dependent optical resonances. Since then, numerous mechanisms have been introduced to manipulate the non-radiative heat exchanges¹⁰⁻¹³ between two bodies. Recently, a far-field thermal rectifier has been proposed on the basis of spectrally selective micro or nanostructured thermal emitters¹⁴ as previously developed to design coherent thermal sources¹⁵ and to enhance the near-field thermal emission of composite structures.¹⁶ However, so far only relatively weak radiative and non-radiative thermal rectifications have been highlighted with these mechanisms ($\eta < 44\%$ in Refs. 8 and 9, $\eta < 52\%$ in Ref. 12, and $\eta < 70\%$ in Ref. 14 for instance).

In this letter, we propose a radiative thermal rectification principle based on the phase transition of insulator-metal transition (IMT) materials around the operating temperature.

In an IMT material a small smooth change of the temperature around its critical temperature T_c causes a sudden qualitative and quantitative change in its optical properties.¹⁷ In a recent work, van Zwol *et al.* have shown that the near-field heat-flux exchanged between two media, at close separation distances (subwavelength), could be modulated by several orders of magnitude across the phase transition of vanadium dioxide (VO₂) deposited on one of the surfaces.¹¹ Here the concept of a far-field radiative thermal rectifier is presented. We show that the drastic change in the optical behavior of IMT material across the phase transition between its amorphous and its crystalline phase can lead to a thermal rectification coefficient which is greater than 70% for small temperature differences and can even be larger than 90% making these devices serious candidates for thermal diodes without any contact between the high and the low temperature regions.

To start, let us consider a system as illustrated in Fig. 1, where two semi-infinite plane bodies, one made of VO₂ and

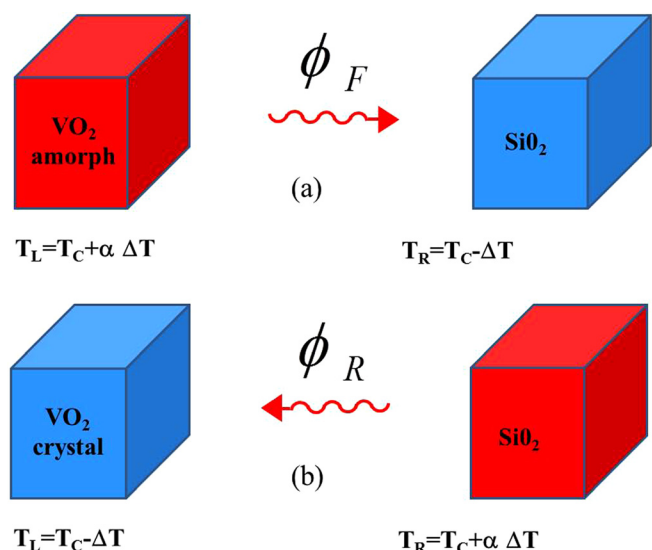


FIG. 1. Schematic of a phase-change radiative thermal diode. (a) Forward scenario: the phase-change material is in its amorph state at higher temperature than its transition temperature T_c . (b) Reverse scenario: the phase change material is in its crystalline state.

^{a)}Electronic mail: pba@institutoptique.fr

^{b)}Electronic mail: s.age.biehs@uni-oldenburg.de

one made of amorphous glass (SiO_2) at temperatures T_L and T_R , respectively. Both media are separated by a vacuum gap of thickness d which is assumed to be much larger than their thermal wavelengths so that heat exchanges are mainly due to propagating photons, i.e., we are considering the far-field regime. We now examine this system in the two following thermal operating modes: (i) In the forward mode (F) the temperature $T_L = T_c + \alpha\Delta T$ of VO_2 is greater than its critical temperature $T_c = 340\text{K}$ so that VO_2 is in its metallic phase while the temperature of the glass medium is $T_R = T_c - \Delta T < T_L$. The average temperature can be either positioned at T_c (i.e., $\alpha = 1$) or shifted to lower or higher values. (ii) In the reverse mode (R) $T_L = T_c - \Delta T$ so that VO_2 is in its crystalline phase and $T_R = T_c + \alpha\Delta T > T_L$. In its crystalline (monoclinic) phase, VO_2 behaves as a uniaxial medium. Experimental data show that¹⁷ the optical axis of VO_2 films is orthogonal its surface [see Fig. 2 for a plot of the permittivities parallel and perpendicular to the surface]. The net heat flux exchanged per unit surface between two isotropic media or between one uniaxial and one isotropic medium can be written in the general form^{18–20}

$$\begin{aligned}\Phi_{F/R} &= \int_0^\infty \frac{d\omega}{2\pi} \Delta\Theta(\omega) \sum_{j=\{s,p\}} \int \frac{d^2\boldsymbol{\kappa}}{(2\pi)^2} \mathcal{T}_{j,F/R}(\omega, \boldsymbol{\kappa}; d), \\ &= \int_0^\infty d\omega \Delta\Theta(\omega) \varphi_{F/R}(\omega, d),\end{aligned}\quad (1)$$

where $\Delta\Theta(\omega) = \Theta(\omega, T_L) - \Theta(\omega, T_R)$ is the difference of mean energies of Planck oscillators at frequency ω and at the temperatures of two interacting media. As for $\mathcal{T}_{j,F/R}(\omega, \boldsymbol{\kappa})$ represents the energy transmission probability carried by the mode $(\omega, \boldsymbol{\kappa})$ ($\boldsymbol{\kappa}$ is the lateral wave vector) in one of two polarization states (s and p polarization). It is defined for the propagating modes with $\kappa < \omega/c$ by²¹

$$\mathcal{T}_{j,F/R}(\omega, \boldsymbol{\kappa}; d) = \text{Tr}[(1 - \mathbb{R}_2^\dagger \mathbb{R}_2) \mathbb{D}^{12} (1 - \mathbb{R}_1^\dagger \mathbb{R}_1) \mathbb{D}^{12\dagger}],\quad (2)$$

where the reflection matrix of each interface is given by ($l = 1, 2$)

$$\mathbb{R}_l = \begin{bmatrix} r_l^{s,s}(\omega, \kappa) & r_l^{s,p}(\omega, \kappa) \\ r_l^{p,s}(\omega, \kappa) & r_l^{p,p}(\omega, \kappa) \end{bmatrix},\quad (3)$$

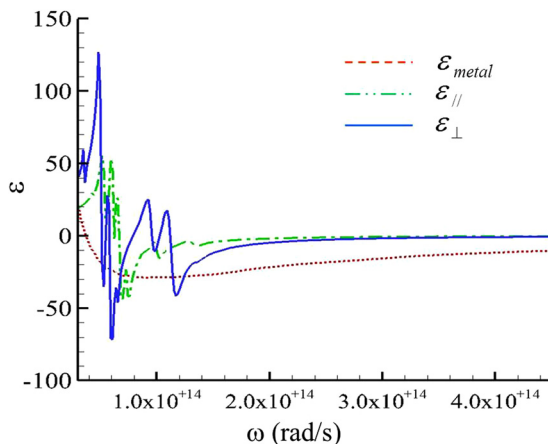


FIG. 2. Permittivities of VO_2 in the metallic phase (ϵ_{metal}) and in the crystalline phase (ϵ_{\parallel} and ϵ_{\perp}).

and the matrix \mathbb{D}^{12} is defined as

$$\mathbb{D}^{12} = (1 - \mathbb{R}_1 \mathbb{R}_2 e^{2ik_{z0}d})^{-1},\quad (4)$$

with $k_{z0} = \sqrt{\omega^2/c^2 - \kappa^2}$. The matrix elements $r_l^{j'j}$ of the reflection matrix are the reflection coefficients for the scattering of an incoming j -polarized plane wave into an outgoing j' -polarized wave. For isotropic or uniaxial media with the optical axis orthogonal to the surface $r_l^{s,p} = r_l^{p,s} = 0$. The remaining reflection coefficients are given by

$$r_l^{s,s} = \frac{k_{z0} - k_{l,s}}{k_{z0} + k_{l,s}},\quad (5)$$

$$r_l^{p,p} = \frac{\epsilon_{\parallel} k_{z0} - k_{l,p}}{\epsilon_{\parallel} k_{z0} + k_{l,p}},\quad (6)$$

where $k_{l,s,p}$ are solutions of the Fresnel equation

$$\left(\epsilon_{\parallel} \frac{\omega^2}{c^2} - \kappa^2 - k_{l,s}^2 \right) \left(\epsilon_{\parallel} \epsilon_{\perp} \frac{\omega^2}{c^2} - \epsilon_{\parallel} \kappa^2 - \epsilon_{\perp} k_{l,p}^2 \right) = 0.\quad (7)$$

Here ϵ_{\parallel} and ϵ_{\perp} are the permittivities parallel and perpendicular to the surface of the uniaxial material VO_2 . For amorphous glass which is isotropic we have $\epsilon_{\parallel} = \epsilon_{\perp} = \epsilon_{\text{SiO}_2}$.²² Finally, we simplify the above expressions for the transmission coefficients by taking the limit $d \rightarrow \infty$ and obtain

$$\mathcal{T}_{j,F/R}(\omega, \kappa) = \frac{(1 - |r_1^{jj}(\omega, \kappa)|^2)(1 - |r_2^{jj}(\omega, \kappa)|^2)}{1 - |r_1^{jj}(\omega, \kappa)|^2 |r_2^{jj}(\omega, \kappa)|^2}.\quad (8)$$

Figures 3(a) and 3(b) show the flux exchanged in the far field for the forward and the reversed scenario with respect to the temperature difference and the degree of asymmetry of the temperature gradient. The evolution of fluxes Φ_F and Φ_R are very similar (they increase monotonically with the temperature difference). In the forward scenario, the magnitude of the flux is always more than 10 times greater than in the reverse scenario. In order to understand this difference, we have plotted in Fig. 4 the spectral heat flux $\varphi(\omega, d \rightarrow \infty)$ defined in Eq. (1) using the transmission coefficient in Eq. (8) for the forward and reversed scenario. With amorphous VO_2 , the spectral heat flux is broadband and scales like $\propto \omega^2$ beyond $\omega = 2.2 \times 10^{14}$ rad/s that is in the frequency range where the diode operates when $T_L > T_c$. On the contrary, when VO_2 is crystalline, all propagating modes located at frequencies greater than $\omega = 1.5 \times 10^{14}$ rad/s give a very small and nearly constant contribution to the spectral heat flux and therefore do not transport much energy. This comes from the weak emissivity of VO_2 in this state. Hence, VO_2 changes for frequencies larger than approximately $\omega = 1.5 \times 10^{14}$ rad/s from a metallic broadband emitter in the forward scenario to a very strong reflector (and hence very poor thermal emitter) in the reverse configuration. This asymmetry is the key for obtaining a highly efficient phase-change thermal diode.

The rectification coefficient η of this rectifier is plotted in Fig. 5. For very small temperature differences we find that $\eta \simeq 70\%$ illustrating the high efficiency of the phase transition of VO_2 . This coefficient grows to $\sim 92\%$ for large temperature differences $\Delta T = 200$ and for a large asymmetry

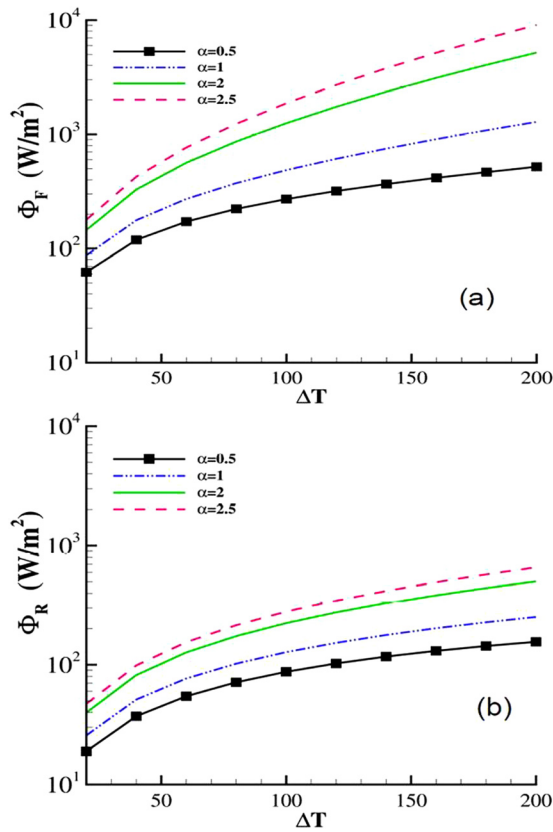


FIG. 3. Orientation dependence of heat flux in (a) the forward and (b) in the reversed temperature scenario between VO₂ and glass. The dielectric permittivities of glass and VO₂ are taken from Refs. 17 and 22 while the critical transition temperature of VO₂ is $T_c = 340\text{ K}$.

factor of $\alpha = 2.5$. On the contrary, when α is small the thermal rectification does not grow significantly with ΔT . In such a configuration, the distribution function involves the modes of high frequencies in the forward scenario and the modes of low frequency in the reverse scenario. But, according to Fig. 3, the efficiency of heat transport by these modes is relatively high in both cases. As consequence, the flux exchanged in both scenarios is similar as we see in Fig. 2.

In conclusion, we have introduced the concept of a phase-change radiative rectifier. Thanks to the bifurcation

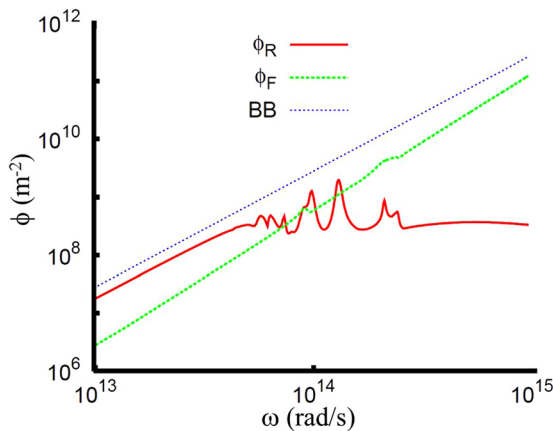


FIG. 4. Plot of the spectral heat flux $\varphi_{F/R}(\omega, d \rightarrow \infty)$ introduced in Eq. (1) as a function of frequency for forward direction where VO₂ is metallic and the reverse situation where VO₂ is crystalline. In addition, we have plotted $\varphi = \frac{\omega^2}{\pi^2 c^3} \epsilon$ for the case that both materials are perfect black bodies, i.e., $T_{jR/F} = 1$.

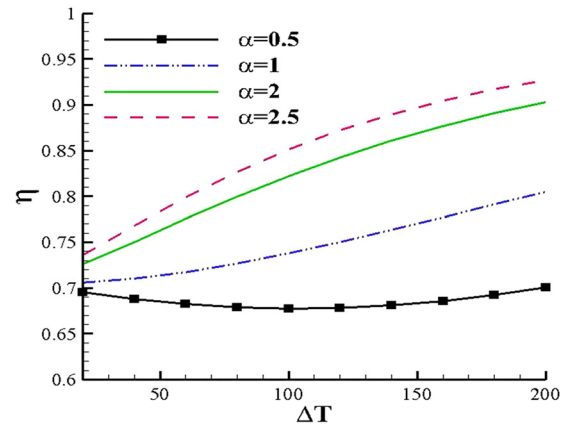


FIG. 5. Rectification coefficient of a VO₂-glass system with respect to the temperature discrepancy and the asymmetry of temperature gradient compared with the critical temperature T_c .

in the optical behavior of MITs close to the critical temperature, large thermal rectification coefficients can be obtained. The here obtained rectification coefficients are between 70% and 92% which is rather high as compared to previous radiative rectifier concepts which show rectification coefficients less than 44%, 52%, or 70%.^{8,9,12,14} Hence, by means of using phase change materials, very efficient thermal diodes can be designed. Beyond their potential for thermal management, these radiative thermal rectifiers suggest the possibility to develop out of contact thermal analogs of electronic devices such as radiative thermal transistors and radiative thermal memories for processing information by utilizing photons rather than electrons and thermal sources rather than electric currents.

¹C. Starr, *J. Appl. Phys.* **7**, 15 (1936).
²N. A. Roberts and D. G. Walker, *Int. J. Therm. Sci.* **50**, 648 (2011).
³N. Li, J. Ren, L. Wang, G. Zhang, P. Hänggi, and B. Li, *Rev. Mod. Phys.* **84**, 1045–1066 (2012).
⁴B. Li, L. Wang, and G. Casati, *Phys. Rev. Lett.* **93**, 184301 (2004).
⁵D. Segal, *Phys. Rev. Lett.* **100**, 105901 (2008).
⁶H.-Y. Cao, H. Xiang, and X.-G. Gong, *Solid State Commun.* **152**, 1807–1810 (2012).
⁷M. J. Martínez-Pérez and F. Giazotto, *Appl. Phys. Lett.* **102**, 182602 (2013).
⁸C. R. Otey, W. T. Lau, and S. Fan, *Phys. Rev. Lett.* **104**, 154301 (2010).
⁹H. Iizuka and S. Fan, *J. Appl. Phys.* **112**, 024304 (2012).
¹⁰S.-A. Biehs, F. S. S. Rosa, and P. Ben-Abdallah, *Appl. Phys. Lett.* **98**, 243102 (2011).
¹¹P. J. van Zwol, K. Joulain, P. Ben-Abdallah, and J. Chevrier, *Phys. Rev. B* **84**, 161413(R) (2011).
¹²S. Basu and M. Francoeur, *Appl. Phys. Lett.* **98**, 113106 (2011).
¹³L. Zhu, C. R. Otey, and S. Fan, *Appl. Phys. Lett.* **100**, 044104 (2012).
¹⁴E. Nefzaoui, J. Drevillon, Y. Ezzahri, and K. Joulain, e-print [arXiv:1306.6209v1](https://arxiv.org/abs/1306.6209v1).
¹⁵J. Drevillon, K. Joulain, P. Ben-Abdallah, and E. Nefzaoui, *J. Appl. Phys.* **109**, 034315 (2011).
¹⁶P. Ben-Abdallah, K. Joulain, J. Drevillon, and G. Domingues, *Appl. Phys. Lett.* **94**, 153117 (2009).
¹⁷A. S. Barker, H. W. Verleur, and H. J. Guggenheim, *Phys. Rev. Lett.* **17**, 1286 (1966).
¹⁸D. Polder and M. Van Hove, *Phys. Rev. B* **4**, 3303 (1971).
¹⁹S.-A. Biehs, E. Rousseau, and J.-J. Greffet, *Phys. Rev. Lett.* **105**, 234301 (2010).
²⁰P. Ben-Abdallah and K. Joulain, *Phys. Rev. B* **82**, 121419(R) (2010).
²¹S.-A. Biehs, P. Ben-Abdallah, F. S. S. Rosa, K. Joulain, and J.-J. Greffet, *Opt. Express* **19**, A1088–A1103 (2011).
²²*Handbook of Optical Constants of Solids*, edited by E. Palik (Academic Press, New York, 1998).